

ON THE ROLE OF INLET FLOW INSTABILITIES ON HORIZONTAL INITIALLY STRATIFIED LIQUID-LIQUID FLOW DEVELOPMENT

Morgan R.G., Ibarra R., Zadrazil I.* and Markides C.N.

*Author for correspondence

Department of Chemical Engineering,
 Imperial College London,
 London, SW7 2AZ,
 United Kingdom,

E-mail: i.zadrazil06@imperial.ac.uk

ABSTRACT

For a given pair of fluid phases, liquid-liquid flows are generally described in terms of regimes (e.g. stratified, wavy or dispersed), which are a function of the Reynolds numbers of the individual phases, the geometry of the flow, as well as the inlet conditions and the distance from the inlet. Typically, injecting the heavier phase at the bottom of the channel and the lighter phase at the top is the common inlet configuration when establishing a liquid-liquid flow for study in a laboratory environment. This configuration corresponds to that expected in a naturally separated flow orientation, on the assumption that at long lengths the density difference between the two phases will lead to this arrangement of the two phases. In this study, a series of experiments were designed to investigate the influence of injecting the heavier phase at the top of the pipe rather than at the bottom. This modification introduces the possibility of phase breakup near the inlet by an additional instability mechanism (due to the density difference between the two liquids), which would not appear had the phases been introduced in the conventional inlet flow arrangement. We perform detailed flow measurements and observe that this flow arrangement gives rise to altered flow structures downstream. Moreover, our results suggest that the effects of this instability near the inlet may persist along the pipe and influence the observed flow behaviour even at long lengths.

INTRODUCTION

The fundamental understanding, prediction and characterisation of liquid-liquid flows represents a major scientific challenge, due to the inherent complexity, multiscale nature and nonlinear behaviour of these flows. Beyond their fundamental importance, the investigation of these flows is highly relevant for the industrial sector, e.g. the petroleum industry where oil and water mixtures are transported in

pipelines, extrusion flows in the polymer industry, mixing of immiscible liquids in the chemical production industry, the power sector, as well as in various pharmaceutical processes.

NOMENCLATURE

A	[m]	Cross-sectional area
D	[m]	Pipe diameter
H	[m]	Interface level
m	[-]	Ratio of dynamic viscosities
Re	[-]	Reynolds number
U	[m.s ⁻¹]	Velocity
Special characters		
μ	[Pa.s]	Dynamic viscosity, also mean
σ	[-]	Standard deviation
ϕ_{in}	[-]	Oil input fraction
$\phi_{mod,1}$	[-]	In-situ oil fraction predicted by laminar drag model
$\phi_{mod,2}$	[-]	In-situ oil fraction predicted by differential momentum balance model
$\langle \phi \rangle_{y,t}$	[-]	In-situ oil phase fraction
Subscripts		
gs		Glycerol solution (with water)
m		Mixture

This present paper focuses on co-current flows of two immiscible liquid phases in a horizontal round pipe. The investigated flows develop from a fully stratified inlet section, where the fluids are introduced with the heavier liquid flowing over the lighter one. Depending on the diameter of the pipe, the ratios of the inlet flow areas occupied by the two fluid phases, the flow rates of the two fluids, it is expected that a range of flow regimes can emerge (e.g. stratified, wavy or dispersed), which are also a function of the distance from the inlet. This paper investigates the effect of the inlet flow condition on the

flow downstream, and attempts to determine whether the flow becomes fully developed at the measurement point.

The typical inlet configuration when establishing a liquid-liquid flow for study in a laboratory environment involves injecting the heavier liquid phase at the bottom of the pipe and the lighter phase at the top. This arrangement is motivated by the need to establish fully developed flow behaviour at the shortest possible lengths, on the assumption that at long lengths the density difference between the two phases will lead naturally to this final arrangement of the two phases.

Fully developed (long-length) horizontal liquid-liquid flow behaviour, however, may not be the same in the case where the inlet flow arrangement changes such that the heavy phase is initially flowing over the lighter one. This would result from the generation of different stable flow features initially in the flow, caused by additional phase breakup mechanisms, which may not evolve to the same final flow state. In particular, the augmented phase breakup and resulting flow structures may arise from additional instabilities in the flow, such as those related to the density difference between the two phases. We will refer to this instability mechanism as the Rayleigh-Taylor instability, or RT instability. This instability mechanism is expected to be significant when the heavier fluid flows above a lighter fluid, because gravity forces will act to make the heavier liquid sink and displace the lighter fluid to the top of the pipe.

In addition to considerations of density, in low Reynolds number (Re) stratified flows, the viscous forces dominate the flow, resulting in smooth laminar flow. When the inertial forces overcome the viscous forces, the flow becomes turbulent leading to instabilities at the interface, and consequent phase mixing. The present study covers Reynolds numbers spanning the ranges 240 – 5,080 for the oil phase and 20 – 370 for the aqueous phase. Two main mechanisms for mixing in the liquid-liquid flow can be present in the investigated flows: due to enhanced turbulence at the higher Reynolds numbers and due to the RT instability as discussed above.

Liquid-liquid flow characterisation is commonly performed on measurements of integral parameters (such as pressure drop) and qualitative flow observations. In this study, advanced flow visualisation techniques are used to investigate the flow hydrodynamics in detail, namely, Planar Laser Induced Fluorescence (PLIF), Particle Image Velocimetry (PIV) and Particle Tracking Velocimetry (PTV). The resulting PLIF images are used to inspect the topological features of the oil and water phases, as well as to obtain information for a statistical analysis of the phase distributions and droplet sizes. On the other hand, the PIV and PTV data are used to provide velocity vectors and velocity profiles in the two phases.

The PIV/PTV measurements are achieved by tracking particles in the flow, which are captured by a high-speed camera that is synchronised with the laser sheet. These advanced visualisation techniques require that the refractive indices between the two liquids are matched. In addition, for the PLIF measurements a fluorescent dyestuff is added to one of the phases (the aqueous/glycerol solution phase). This dyestuff is excited by the laser light and re-emits light indicating the presence of the phase in which it has been added.

In a recent study [1,2], PLIF and PIV/PTV were employed to measure co-current horizontal liquid-liquid flows in the same circular pipe section, with the lighter phase introduced over the heavier one. Images were processed to obtain flow regime information, vertical phase distributions, in situ phase fraction, interface level, drop size distributions, and velocity profiles. The current study extends the previous mentioned work to investigate the effect of imposing a RT instability at the inlet.

EXPERIMENTAL METHODS

Experimental investigations were carried out in the Two-Phase Oil-Water Experimental Rig (or, TOWER) located at Imperial College London. A schematic of the test facility is shown in Figure 1. The test section consists of a 1-in. ($D = 25.4$ mm) nominal bore stainless steel circular pipe with a total length of 7.30 m. The visualisation cell was positioned at a distance of 6.20 m from the inlet and consisted of a circular cross-section borosilicate glass tube housed in a Perspex box. The test fluids used in the experimental investigation were an aliphatic hydrocarbon oil (Exxsol D80) and an aqueous glycerol solution.

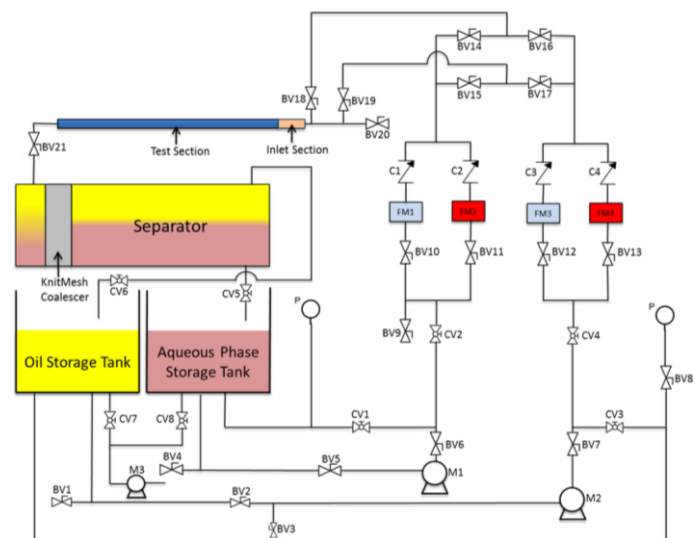


Figure 1 Schematic of the TOWER flow facility used in the present experimental campaign.

Two Grundfos CRN 10-5 pumps were used for the liquid phases. The pumps have a maximum rated flow rate of 2.8 L/s and a maximum rated pressure of 3.60 bar. The flow rates were measured by means of four NB liquid turbine flowmeters, fitted with a Fluid Well FIIQ-X LCD digital display. The flow rates were time-logged onto a computer by means of a 4–20 mA linear current output. Each fluid was directed through one of two turbine flowmeters. The orientation of this arrangement is illustrated schematically in Figure 1. The two flowmeters for each fluid have different measurement flow rate ranges: 2–20 L/min and 14–140 L/min, denoted by FM1 and FM2 respectively. The accuracy of the NB liquid flow is $\pm 0.5\%$, while their repeatability is $\pm 0.1\%$ of full scale.

The superficial mixture velocity U_m , defined as the total volumetric flow rate of both phases divided by the total pipe cross-sectional flow area A , and the oil input fraction ϕ_m , defined as the ratio of the two volumetric flow rates at the inlet, together define the flow condition. In this work, these two independent flow parameters were varied in 48 test runs. The experimental runs spanned a range of superficial mixture velocities from 0.11 to 0.84 m/s and oil input fractions from 0.1 to 0.9. The quantitative analysis of the results focused on the superficial mixture velocity range $U_m = 0.11$ to 0.42 m/s, in order to capture the development of stratified flow to dual continuous flow and to enhance our understanding of the mechanisms driving this flow regime transition. The inlet was configured to inject the glycerol solution above the oil, thus inducing the necessary density difference (and triggering the relevant instability) in the flow as shown in Figure 2.

Optical Measurement Techniques

PLIF was employed to obtain high-quality images, allowing the characterisation of the complex interfacial topology in the flow formed by the two immiscible liquids. Application of this technique requires the matching of the refractive indices of the fluids and pipe to eliminate distortions of the laser sheet. The methods by which this was endured are explained in detail in Refs. [1,2].

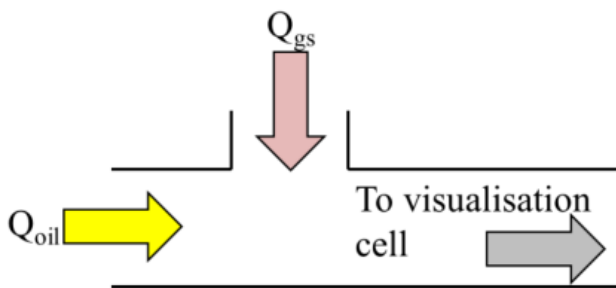


Figure 2 Inlet configuration used in the current study.

The axial velocity components in the visualisation plane were obtained from the PIV and PTV techniques. In this study, micro-droplets were used as tracer particles. Both techniques were used to obtain velocity maps by correlating the position of particles within the flow between successive images.

An Oxford Lasers LS20-10 pulsed copper vapour laser with a nominal output power of 20 W and an internal clock frequency of 10 kHz was used as the green light source for the experimental investigations. The output light spectrum exhibits a peak at 510.6 nm, has a pulse duration of 2 ns and a pulse energy of approximately 2 mJ.

The flow was recorded at either 1 or 2 kHz, depending on the flow rate. A dedicated light sheet generator produced by Oxford Lasers was connected to the copper vapour laser by means of a fibre optic cable. The resulting laser sheet had a thickness of less than 1 mm and a throw distance of 155 mm. The configuration of the laser sheet setup is shown in Figure 3. Fluorescent images from the laser illumination of the test section were video recorded using an iSpeed3 high-speed video cameras produced by Olympus. The camera has a maximum

resolution of 1280 x 1024 pixels at which the maximum attainable frame-rate is 2000 fps. The actual imaging frequency employed in the current measurements was set by the laser repetition frequency, which was either 1 or 2 kHz. A Macro 105 mm F2.8 EX DG medium telephoto lens produced by Sigma Imaging Ltd was used for the imaging.

The output pulse of the copper vapour laser was synchronised with the camera system to ensure that the laser produced pulses during the exposure of the camera and that the camera captured the resulting laser-induced fluorescence. A trigger box employing TTL (transistor–transistor logic) signals was used to synchronise the laser with the camera. The trigger box was driven by a frame-rate signal outputted from the camera. From the trigger box a signal was then sent to the laser. The signal reduced the pulse repetition frequency of the laser from its internal clock frequency of 10 kHz to the frequency the camera was set to, for as long as the camera was allowed to capture images.

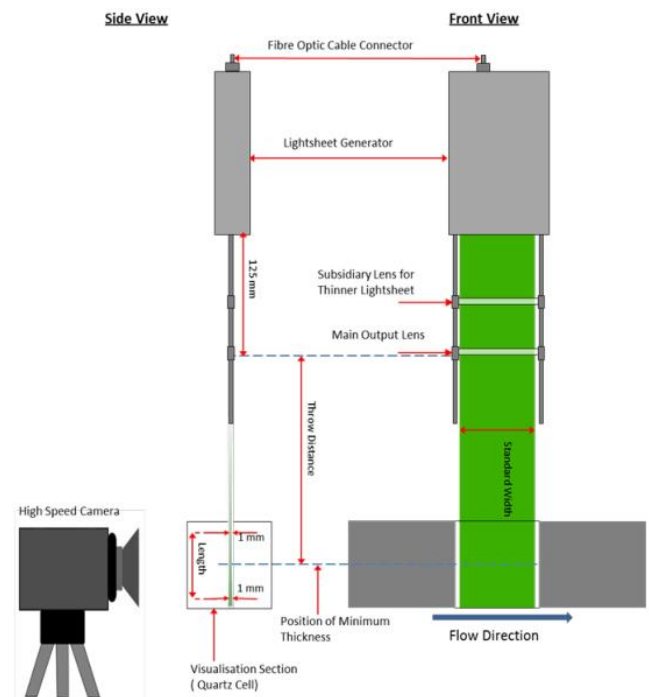


Figure 3 Laser sheet setup and camera arrangement.

Fluid Selection

The test fluids used were an aliphatic hydrocarbon oil (Exxsol D80) and a glycerol solution. The determination of the glycerol solution concentration was based on refractive indices matching with the oil phase. The concentration of the final glycerol-water solution was determined by taking into account the effect of the dyestuff added to the aqueous solution. The fluorescent dyestuff maximise the brightness of the aqueous phase to obtain clear images. It was found an optimal concentration of 0.4 mL of Eosin Y solution (5 wt.%) per litre of aqueous solution.

An Abbe 60 Refractometer was used to measure the refractive indices of the fluids. The refractive index of the

Exxsol D80 at 20°C was found to be 1.444. A glycerol solution of 81.7 wt.% with 0.4 mL/L of Eosin Y matched the refractive index of the Exxsol D80 to 3 decimal points. This allows the implementation of optical visualisation techniques with no distortions. The physical properties of the test fluids are shown in Table 1.

Table 1 Fluids physical properties at 20°C.

	Exxsol D80	Glycerol solution 81.7 wt.% with 0.4mL/L of Eosin Y at 5 wt.%
Density (kg/m ³)	802.7	1213.3
Viscosity (mPa.s)	1.9	82.3
Refractive index	1.444	1.444

The fluids have comparable properties to those found in previous works. The two liquid used in the current experimental investigations were the same as those used in earlier studies [2,3]. The oil has identical properties to the oils used by [4,5]. The density ratio between the oil and glycerol solution is 1.5, which is comparable to density ratios of previous studies [6-9]. In addition, the fluids have a viscosity ratio (aqueous glycerol solution to oil) of approximately 20, which is comparable to the viscosity ratios of previous studies [7,10]. However, for the majority of the previous experimental work the oil is the less dense and more viscous fluid, while in the current study the oil is the less dense and also the less viscous fluid.

Graticule Image Correction Technique

Image distortion from the optical techniques occurs when the laser sheet pass through the circular walls of the test pipe at the visualisation cell. This problem can be avoided by using a pipe material with the same refractive index as the fluids. However, the pipe material that most closely matched the refractive index and being suitable for flow visualisation (i.e. transparent, sufficient strength/rigidity, chemical compatible with the test fluids) was borosilicate glass with a refractive index of 1.474. As a result, a graticule correction technique was employed to account for the distortion on the laser sheet.

Before and after each set of experimental runs a graticule calibration piece was inserted into the visualisation cell. The cell was detached of the test section and filled with Exxsol D80. The known sizes and spacing of the graticule calibration piece were used to measure the displacement and distortion when the image is captured by the camera. A correlation was found based on the discrepancy between the generated image and the known position of the graticule calibration piece. The operation was performed using existing algorithms in the DaVis software package produced by LaVision.

RESULTS

A flow regime map for the experimental flow conditions is presented in Figure 4 as a function of the varied independent variables in the present study, which are the superficial mixture

velocity and oil input fraction. The flow regime map is in good agreement with those presented previous by various researchers in the literature [4,5,11]. However, comparison with results acquired for aqueous phase injected at the bottom of channel [2] shows that the stratified flow with droplets regime is seen at both lower mixture velocities (0.17 m/s opposed to 0.22 m/s) and lower oil input fractions. In addition, oil droplets are more prevalent and the oil droplet layer flow regime is observed across a broader range of flow conditions.

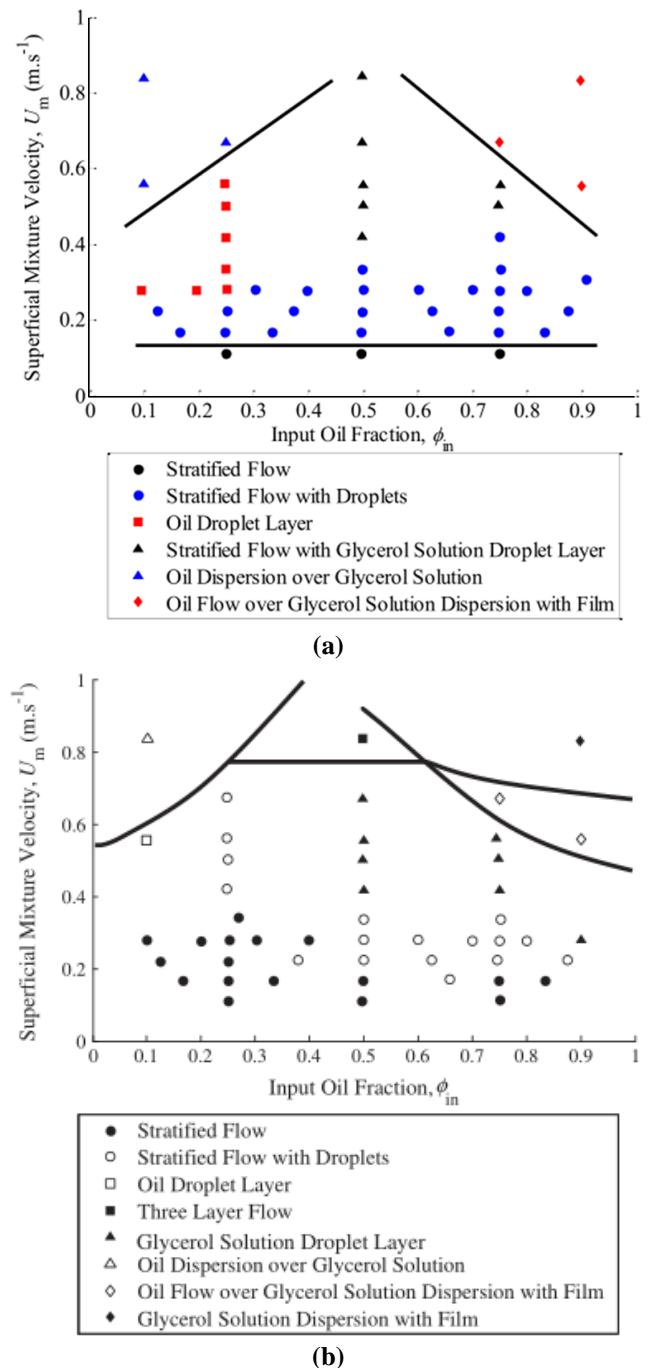


Figure 4 Flow regime maps: (a) from the present study; (b) from the study in Refs. [1,2] relating to the stable inlet fluid arrangement (taken from Ref. [1]).

From our preliminary considerations pertaining to the RT instability and considering the time elapsed from the flow entering the test section to reach the visualisation cell, it was determined that the flow should not be affected by the inlet configuration [1, 12, 13].

However, from the experimental results it can be concluded that the flow is still displaying characteristics different to those observed when the heavier phase is injected at the bottom of the pipe [2], and these differences can be attributed to the “inverted” inlet configuration.

Vertical Phase Distribution Profiles

Three different regions can be observed from the experimental investigations: (1) an oil region; (2) a glycerol solution region, and (3) a mixed region at the interface. For stratified flows, the mixed region appears as a narrow vertical band which increases with the superficial mixture velocity. The height of the mixed band increases as the oil input fraction is increased. The height of the glycerol solution layer at the pipe bottom and the vertical height covered by the mixed region decrease for the above conditions.

A comparison between flow images obtained by injecting

the heavier phase at the bottom of the pipe [2] and the current study are presented in Figure 5. From comparing the “inverted” inlet condition results with the “normal” inlet condition results, it is concluded that the inlet configuration does have an effect on the flow regime at the distance far downstream of the inlet ($L/D = 244$) at which the PLIF-PTIV measurements were taken.

As the superficial mixture velocity increases, the flow behaviour becomes significantly different (Figure 5(b)). This can be potentially explained in terms of the inlet configuration inducing a RT instability leading to more mixing in the flow. Even though enough time has elapsed for the oil droplets to reach the top of the channel, these risen oil droplets have not coalesced to form a continuous oil region at the top. This can be attributed to the viscosity of the glycerol solution, which is significantly higher than the oil phase. As a result, the drainage process of the continuous phase between the droplets becomes slow, retarding the coalescence process.

In-situ Phase Fraction

In-situ oil phase fractions $\langle \phi \rangle_{y,t}$ were calculated by using the phase distribution profiles coupled with a numerical integration technique to account for the curvature of the visualisation cell wall. Figure 6 shows the results for the in-situ oil fraction as a

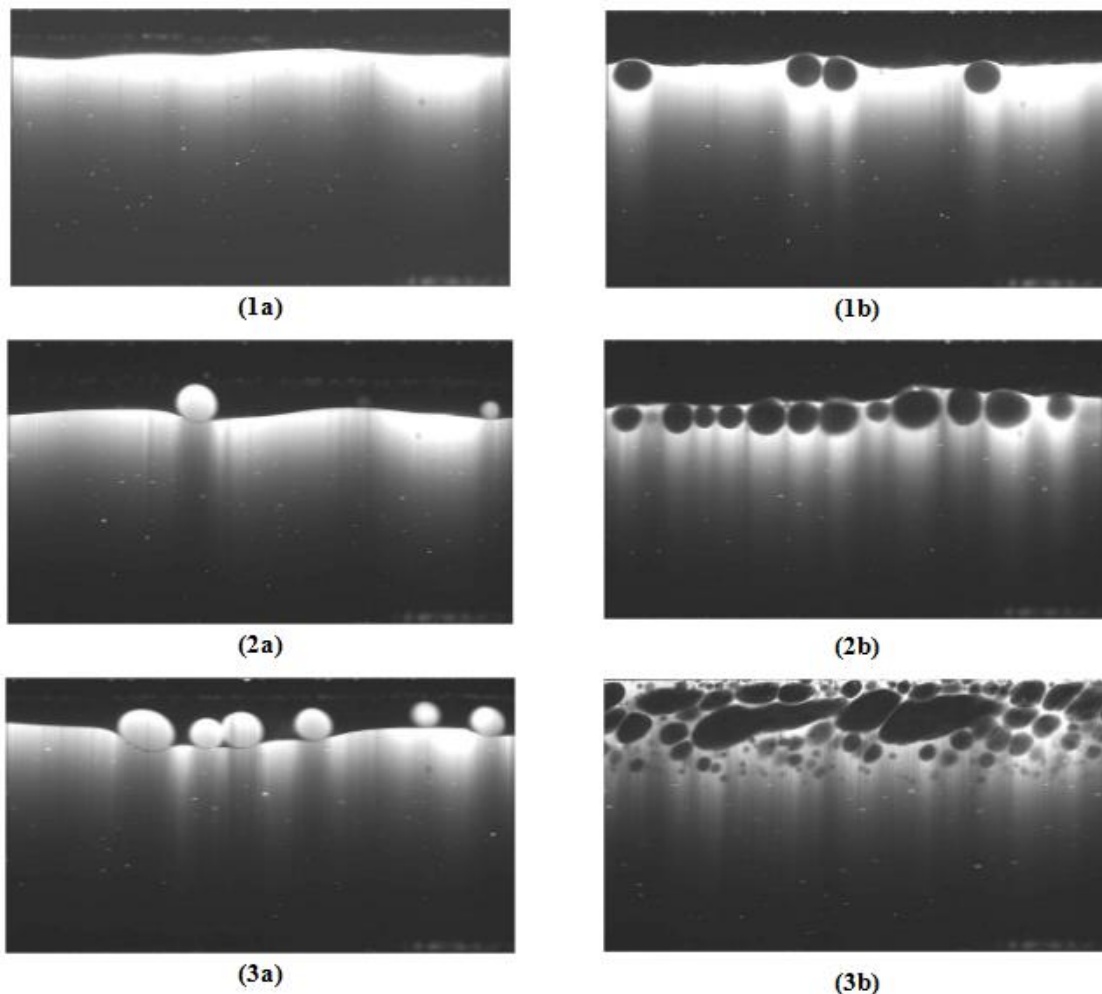


Figure 5 Instantaneous images for: (1) $U_m = 0.17$ m/s and $\phi_n = 0.17$; (2) $U_m = 0.33$ m/s and $\phi_n = 0.25$, and; (3) $U_m = 0.28$ m/s and $\phi_n = 0.1$; “a” refers to the “normal” inlet configuration and “b” to the “inverted” inlet configuration.

function of the oil input fraction and superficial mixture velocity. Results concur with the findings by Morgan et al. (2013) for a “normal” inlet condition. It can be seen that the in-situ oil fraction is lower than the input oil fraction for almost all flow conditions. This is shown in Figure 6 as $S = 1$ (homogeneous flow model) in which no slippage occurs between the fluids.

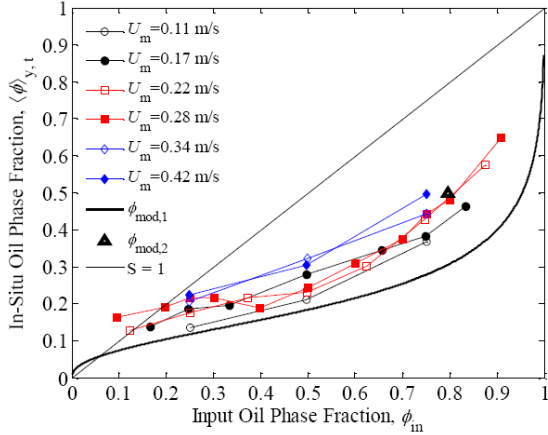


Figure 6 In-situ oil fraction $\langle\phi\rangle_{y,t}$ as function of oil input fraction ϕ_{in} and superficial mixture velocity U_m .

Two models were developed to describe the in-situ oil fraction: (i) laminar drag model denoted by $\phi_{mod,1}$; and (ii) differential momentum balance model denoted by $\phi_{mod,2}$. The laminar drag model was developed by equating the frictional pressure drop in a two-layer flow, i.e. by considering an equilibrium between viscous drag due to laminar flow and pressure drop in the pipe. This model was derived by Morgan et al. (2013) and is presented in equation (1):

$$\phi_{mod,1} = \langle\phi\rangle_{y,t} = \frac{A_{oil}}{A_{oil} + A_{gs}} \quad (1)$$

where A_{oil} and A_{gs} are the cross-sectional area of the oil and glycerol solution, respectively.

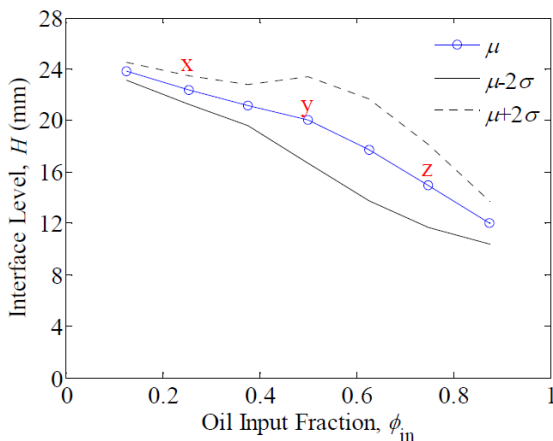


Figure 7 Mean (μ), upper ($\mu + 2\sigma$) and lower ($\mu - 2\sigma$) limits for the interface level H as a function of oil input fraction ϕ_{in} for $U_m = 0.22$ m/s.

The differential momentum balance model is applicable to the special case in which the in-situ oil fraction $\langle\phi\rangle_{y,t} = 0.5$ and when the interface level H is at the midpoint of the pipe. The model is based on the average velocities of each phase. A full derivation is provided in Morgan et al. (2013). Equation (2) shows the differential momentum balance model.

$$\phi_{mod,2} = \langle\phi\rangle_{y,t} = \frac{m + 7}{m + 14 + m^{-1}} \quad (2)$$

where $m = \mu_{gs} / \mu_{oil}$ is the dynamic viscosities ratio of the fluids.

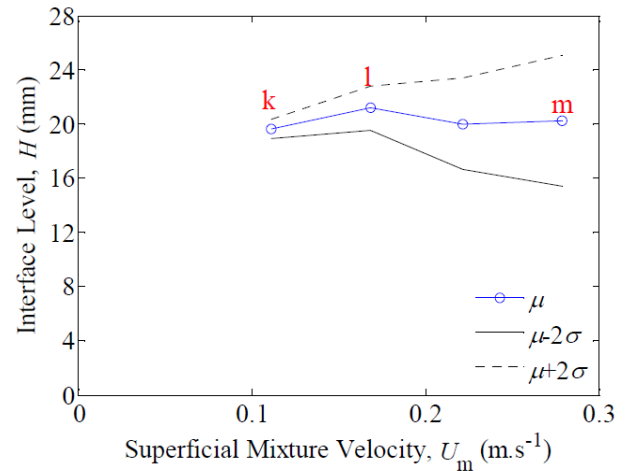


Figure 8 Mean (μ), upper ($\mu + 2\sigma$) and lower ($\mu - 2\sigma$) limits for the interface level H as a function of superficial mixture velocity U_m for $\phi_{in} = 0.50$.

Interface Level

Figure 7 presents the results of the interface level as a function of the oil input fraction for a superficial mixture velocity of $U_m = 0.22$ m/s, while Figure 8 shows the results as a function of the superficial mixture velocity. The interface level reduces as the oil input fraction increases for a given superficial mixture velocity. The fluctuation of the interface level heights increases for an increment in the superficial mixture velocity.

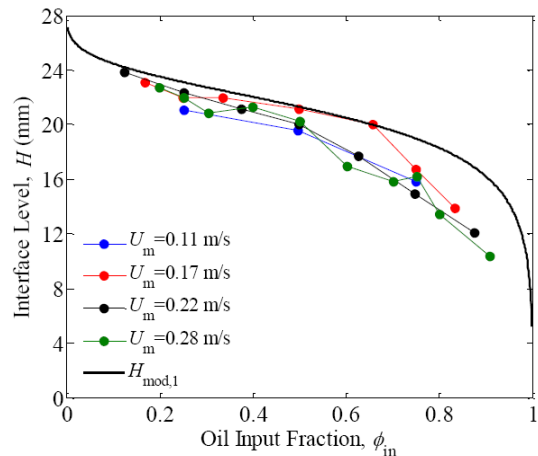


Figure 9 Interface level H as a function of oil input fraction ϕ_{in} for different superficial mixture velocities U_m .

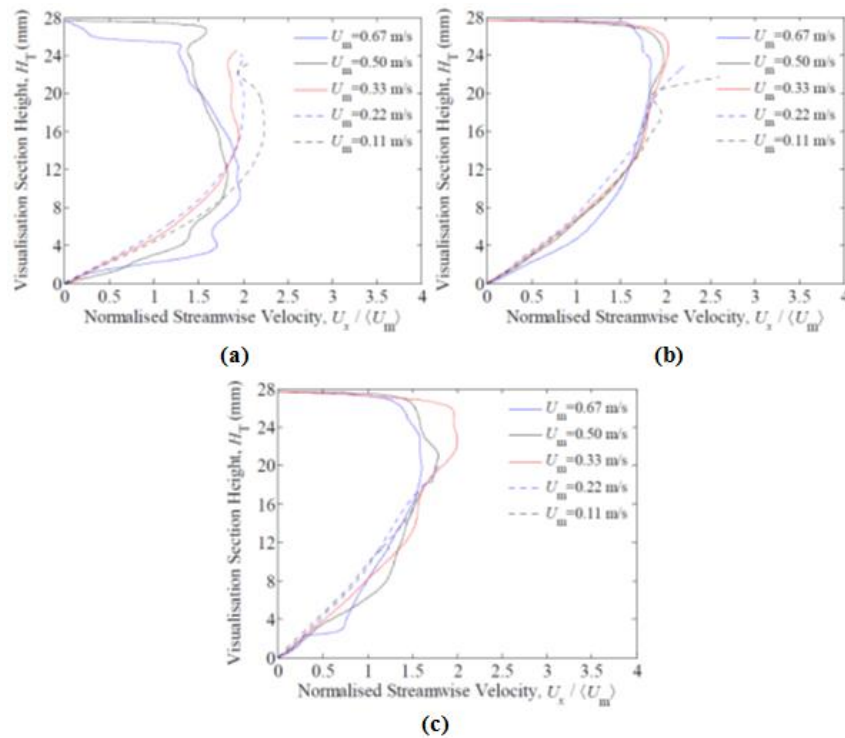


Figure 10 Normalised velocity profiles $U_x / \langle U_m \rangle$ for different superficial velocities and an oil input fraction of: (a) $\phi_n = 0.25$; (b) $\phi_n = 0.50$, and; (c) $\phi_n = 0.75$.

The widening of the upper and lower interface level limits (for the 95% confidence level) with an increasing superficial mixture velocity can be attributed to turbulence. As the superficial mixture velocity increases, the Reynolds number increases, leading to high levels of turbulence. This turbulence can be present as waves at the common interface which can grow in amplitude with the superficial mixture velocity.

Figure presents a comparison of interface levels data with predictions from the laminar drag model (Equation (1)) denoted by $H_{mod,1}$. The laminar drag model has an excellent agreement with the experimental results, specifically for $U_m = 0.17$ m/s. The interface level slightly increases as increasing the superficial mixture velocity for a given oil input fraction from $U_m = 0.11$ to 0.17 m/s. For higher superficial mixture velocities, the interface level decreases. This behaviour can be described by the oil droplet layer below the interface for $U_m \geq 0.17$ m/s for the “inverted” inlet configuration (i.e. injecting the heavier phase at the top of the channel).

Velocity Profiles

Figure 10 shows velocity profiles for superficial mixture velocities between $U_m = 0.11$ to 0.67 m/s and oil input fractions of (a) $\phi_n = 0.25$; (b) $\phi_n = 0.50$, and; (c) $\phi_n = 0.75$. The interface region presents a step change attributed to a velocity difference between the two liquids (i.e. slippage condition). The additional instability for the “inverted” inlet configuration can influence the velocity profiles. However, the velocity profiles for the current study are highly comparable with a “normal” inlet configuration.

Figure 11 presents a velocity profile and an instantaneous image for: (a) stratified flow and (b) dispersed flow. Results are comparable with those for the “normal” inlet configuration. For stratified flow, both phases have Reynolds numbers in the laminar flow region. As a result, a parabolic velocity profile, as seen in Figure 11(a1), is expected. As previously explained, the velocity difference between the two phases creates a step at the interface. The oil phase flows at a higher velocity than the glycerol solution. This velocity difference creates a shift to the right in the velocity profile above the interface.

The step in the velocity profile presented at the interface for stratified flow disappears for dual continuous flow as observed in Figure 11(a2). At significantly high superficial mixture velocities, turbulent intensity increases leading to further mixing of the phases. The velocity profile develops a transition from a parabolic profile (i.e. laminar flow) to a flat profile (i.e. turbulent flow) over the dispersed region.

CONCLUSION

A non-intrusive optical diagnostic technique capable of the high-speed spatiotemporal measurement of liquid phase (with PLIF) and flow velocity distribution (with PTV and PIV) has been applied to acquire measurements of horizontal, initially stratified liquid-liquid flows, with the heavier phase introduced into the measurement pipe above the lighter phase. Exxsol D80 (representing the oil phase) and an aqueous glycerol solution were used as the test fluids with matched refractive indices. A

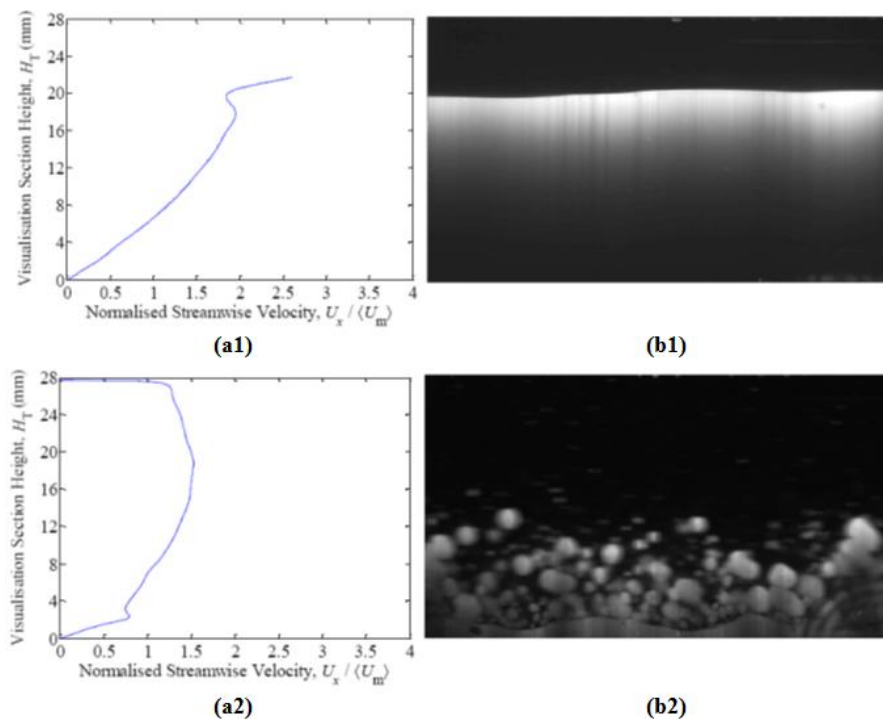


Figure 11 Velocity profiles (a) and instantaneous images (b) for: (1) $U_m = 0.11$ m/s, $\phi_n = 0.50$, and; (2) $U_m = 0.83$ m/s, $\phi_n = 0.90$.

borosilicate glass cell, placed inside a Perspex box, was used to visualise the flow. The image distortion due to the refractive index difference between the glass cell and the fluids was successfully corrected by using a graticule technique.

The flow regimes and general flow behaviour and characteristics in the present study were comparable to those obtained when injecting the heavier phase below the lighter one. However, an increased propensity for the appearance of oil droplets below the interface was observed. From the flow regime map, it was observed that for flows in which roughly equal volumetric flow rates of the two liquids are injected into the pipe, the superficial mixture velocity for transition from stratified flow to other flow regimes (i.e. dual continuous and, in turn, dispersed flow) was higher than that required for this transition for oil input fractions that approach the limits (i.e. $\phi_n = 0$ and 1). This is expected because at $\phi_n \approx 0.5$ flow regime transition is governed by turbulence (i.e. related to Reynolds number). Similar velocity profiles were measured in the current study compared to the experimental results with the heavier phase being injected at the bottom of the pipe.

REFERENCES

- [1] Morgan R.G., Studies of Liquid-Liquid Two-Phase Flows Using Laser-Based Methods, *Ph.D. Thesis, Imperial College London*, 2012
- [2] Morgan R.G., Markides C.N., Zadrazil I., and Hewitt G.F., Characteristics of horizontal liquid-liquid flows in a circular pipe using simultaneous high-speed laser induced fluorescence and particle velocimetry, *International Journal of Multiphase Flow*, Vol. 49, 2013, pp. 99-118
- [3] Morgan R.G., Markides C.N., Hale C.P., and Hewitt G.F., Horizontal liquid-liquid flow characteristics at low superficial velocities using laser induced fluorescence, *International Journal of Multiphase Flow*, Vol. 43, 2012, pp. 101-117
- [4] Soleimani A., Phase Distribution and Associated Phenomena in Oil-Water Flows in Horizontal Tubes, *Ph.D. Thesis, Imperial College London*, 1999
- [5] Hussain S.A., Experimental and Computational Studies of Liquid-Liquid Dispersed Flows, *Ph.D. Thesis, Imperial College London*, 2004
- [6] Russell T.W.F., Hodgson G.W., and Govier G.W., Horizontal pipeline flow of mixtures of oil and water, *Canadian Journal of Chemical Engineering*, Vol. 37, 1959, pp. 9-17
- [7] Charles M.E., and Lilleth L.U., Correlation of pressure gradients for the stratified laminar-turbulent pipeline flow of two immiscible liquids, *Canadian Journal of Chemical Engineering*, Vol. 44, 1966, pp. 47-49
- [8] Simmons M.J.H., and Azzopardi B.J., Drop size distributions in dispersed liquid-liquid pipe flow, *International Journal of Multiphase Flow*, Vol. 27, 2001, pp. 843-859
- [9] Ioannou K., Nydal O.J., and Angeli P., Phase inversion in dispersed liquid-liquid flows, *Experimental Thermal and Fluid Science*, Vol. 29, 2005, pp. 331-339
- [10] Guzhov A.I., Grishin A.D., Medredev V.F., and Medredeva O.P., Emulsion formation during the flow of two liquids in a pipe, *Neft. Khoz.*, Vol. 8, 1973, pp. 58-61 (in Russian)
- [11] Lovick J., and Angeli P., Experimental studies on the dual continuous flow pattern in oil-water flows, *International Journal of Multiphase Flow*, Vol. 30, 2004, pp. 139-157
- [12] Glimm, J., Grove, J.W., Li, X.L. Oh, W. and Sharp, D.H., A critical analysis of Rayleigh-Taylor growth rates, *Journal of Computational Physics*, Vol. 169, 2001, pp. 652-677
- [13] Dimonte, G. and Schneider, M., Density ratio dependence of Rayleigh-Taylor mixing for sustained and impulsive acceleration histories, *Physics of Fluids*, Vol. 12, 2000, pp. 304-332